Ion Energy in Quadrupole Mass Spectrometry

Vladimir Baranov

MDS SCIEX, Concord, Ontario, Canada

Application of an analytical solution of the Mathieu equation in conjunction with algebraic presentation of the Mathieu functions for description of the ion energy in a radiofrequency quadrupole field is discussed in this work. The analytical approach is used to express the ion energy averaged over the initial ion velocity distribution function, field phase and ion residence time. Comparisons with the approximate solutions for potential ion energy are presented with demonstration of their limits. Application of the method for different stability regions is discussed.   (J Am Soc Mass Spectrom 2004, 15, 48-54) © 2004 American Society for Mass Spectrometry

The development of algebraic methods to compute Mathieu functions [1–3] has simplified theoretical description of the motion of ions in a quadrupole field. As a result of this progress, the algebraic aspects of the Mathieu functions were implemented "simply as another special function". The analytical method of the solution of the Mathieu equation in conjunction with algebraic presentation of the Mathieu functions allows introduction of simplifications and generalizations, delivering an alternative method to both the numerical solution of the Mathieu equation and to the matrix method. Previous attempts to use the Mathieu functions were too general due to the absence of simple algorithms or too local due to the necessity to use expansion series around small quantities (see [4] and references therein). The analytical method, in contrast to the matrix method, utilizes a single solution for a complete ion trajectory. The closed formulae obtained provide a general and preferable method for analytical expression of the fundamental properties of the quadrupole field such as ion trajectory stability, transmission/acceptance, resonance (see [5]), and momentum/energy characteristics of the ion motion. The linear quadrupole and the quadrupole trap are considered in this work as examples that demonstrate the advantages of the analytical method for the determination of the fundamental properties of the mass selecting devices as well as their effect on the ion energy. Illustrations of practical implementation of the method are also given for different regions of stability. In this work it is demonstrated that in order to evaluate the average ion energy in the quadrupole RF field, one has to calculate two dimensionless parameters $\upsilon_{21}^2(a, q)$ and $\upsilon_{22}^2(a, q)$, which depend only on the field properties.

Linear Quadrupole

For the two-dimensional quadrupole capacitor, the potential of the RF driven quadrupole field can be expressed as a combination of two terms having spatial (U) and periodic (V) trapping potentials:

$$\Phi = \frac{(x^2 - y^2)}{2r_0^2} (U - V \cos(\omega t + \varphi)), \tag{1}$$

where r_0 is the electrode separation, ω is the main trapping RF angular frequency and φ is the initial phase of the main trapping frequency. In the vicinity of the z-axis, the electrostatic field of such a quadrupole has the equipotential lines forming a hyperbolic surface. That leads us to the system of equations for motion of an ion (with mass m and charge e) having arbitrary initial conditions $\{x_i, y_i, z_i\}$ and $\{\dot{x}_i, \dot{y}_i, \dot{z}_i\}$ (i-initial, $t_i = 0$) in Cartesian system of coordinates:

$$\begin{cases} m\ddot{x}(t) = -e\dfrac{x(t)}{r_0^2}(U - V\cos(\omega t + \varphi)) \\ m\ddot{y}(t) = e\dfrac{y(t)}{r_0^2}(U - V\cos(\omega t + \varphi)), \\ \qquad\quad m\ddot{z}(t) = 0 \end{cases}$$

$$\begin{cases} x(0) = x_i;\ \dot{x}(0) = \dot{x}_i \\ y(0) = y_i;\ \dot{y}(0) = \dot{y}_i \\ z(0) = z_i;\ \dot{z}(0) = \dot{z}_i \end{cases} \tag{2}$$

The properties of the system (eq 2) are as follows: The ion motions in all three directions are independent; axial (z) direction is unaffected by the field; the electric force is linearly proportional to the ion position. Introducing the dimensionless parameters:

$$\frac{4eU}{m\omega^2 r_0^2} = a, \quad \frac{2eV}{m\omega^2 r_0^2} = q,$$

the solution of the equation of motion in the x direction can be presented as:

$$x(t) = \frac{1}{P(a,q)}\left[2\frac{\dot{x}_i}{\omega}Q\left(a,q,\frac{\omega t}{2},\frac{\varphi}{2}\right) + x_i L\left(a,q,\frac{\omega t}{2},\frac{\varphi}{2}\right)\right],$$

$$\dot{x}(t) = \frac{1}{P(a,q)}\left[\dot{x}_i QP\left(a,q,\frac{\omega t}{2},\frac{\varphi}{2}\right) + x_i\frac{\omega}{2} LP\left(a,q,\frac{\omega t}{2},\frac{\varphi}{2}\right)\right]$$

(3)

where

$$Q\left(a,q,\frac{\omega t}{2},\frac{\varphi}{2}\right) =$$

$$C\left(a,q,\frac{\omega t}{2}+\frac{\varphi}{2}\right)S\left(a,q,\frac{\varphi}{2}\right) - C\left(a,q,\frac{\varphi}{2}\right)S\left(a,q,\frac{\omega t}{2}+\frac{\varphi}{2}\right);$$

$$L\left(a,q,\frac{\omega t}{2},\frac{\varphi}{2}\right) =$$

$$\dot{C}\left(a,q,\frac{\varphi}{2}\right)S\left(a,q,\frac{\omega t}{2}+\frac{\varphi}{2}\right) - C\left(a,q,\frac{\omega t}{2}+\frac{\varphi}{2}\right)\dot{S}\left(a,q,\frac{\varphi}{2}\right);$$

$$QP\left(a,q,\frac{\omega t}{2},\frac{\varphi}{2}\right) =$$

$$\dot{C}\left(a,q,\frac{\omega t}{2}+\frac{\varphi}{2}\right)S\left(a,q,\frac{\varphi}{2}\right) - C\left(a,q,\frac{\varphi}{2}\right)\dot{S}\left(a,q,\frac{\omega t}{2}+\frac{\varphi}{2}\right);$$

$$LP\left(a,q,\frac{\omega t}{2},\frac{\varphi}{2}\right) =$$

$$\dot{C}\left(a,q,\frac{\varphi}{2}\right)\dot{S}\left(a,q,\frac{\omega t}{2}+\frac{\varphi}{2}\right) - \dot{C}\left(a,q,\frac{\omega t}{2}+\frac{\varphi}{2}\right)\dot{S}\left(a,q,\frac{\varphi}{2}\right)$$

(4)

and $C\left(a,q,\frac{\omega t}{2}+\frac{\varphi}{2}\right)$ is the even Mathieu function with real characteristic value a and parameter q and $S\left(a,q,\frac{\omega t}{2}+\frac{\varphi}{2}\right)$ is the odd solution. Their derivatives with respect to the $\frac{\omega t}{2}+\frac{\varphi}{2}$ variable are $\dot{C}\left(a,q,\frac{\omega t}{2}+\frac{\varphi}{2}\right)$ and $\dot{S}\left(a,q,\frac{\omega t}{2}+\frac{\varphi}{2}\right)$, respectively. Analogous solutions can be obtained for the y-direction motion converting (a,q) into $(-a,-q)$.

The $P(a,q)$ function is introduced according to the Liouville theorem:

$$\frac{\dot{C}\left(a,q,\frac{\omega t}{2}+\frac{\varphi}{2}\right)S\left(a,q,\frac{\omega t}{2}+\frac{\varphi}{2}\right) - C\left(a,q,\frac{\omega t}{2}+\frac{\varphi}{2}\right)\dot{S}\left(a,q,\frac{\omega t}{2}+\frac{\varphi}{2}\right)}{\dot{C}\left(a,q,\frac{\varphi}{2}\right)S\left(a,q,\frac{\varphi}{2}\right) - C\left(a,q,\frac{\varphi}{2}\right)\dot{S}\left(a,q,\frac{\varphi}{2}\right)} = 1.$$
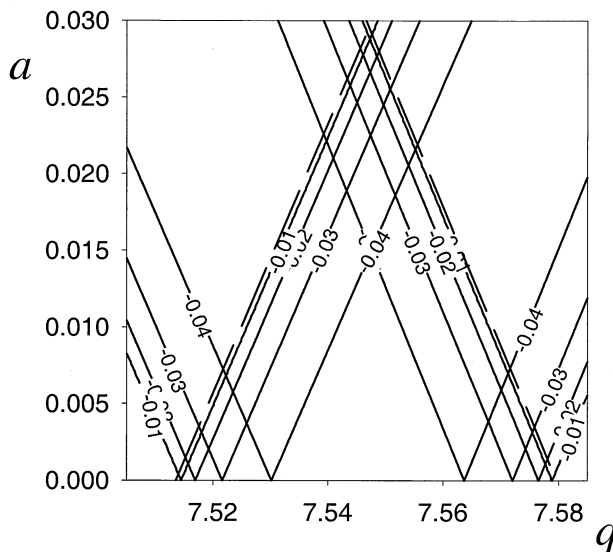

Figure 1. Diagram of stability of ion trajectories in the linear quadrupole for the second stability region calculated employing the $P(a,q)$ function (see eq 5). Dashed lines represent $P(a,q) = 0$. The boundaries computed using the equivalence of the Mathieu characteristic exponent to 0 or an integer number coincide with the $P(a,q) = 0$ boundaries.

Therefore:

$$\dot{C}\left(a,q,\frac{\omega t}{2}+\frac{\varphi}{2}\right)S\left(a,q,\frac{\omega t}{2}+\frac{\varphi}{2}\right) -$$

$$C\left(a,q,\frac{\omega t}{2}+\frac{\varphi}{2}\right)\dot{S}\left(a,q,\frac{\omega t}{2}+\frac{\varphi}{2}\right) =$$

$$\dot{C}\left(a,q,\frac{\varphi}{2}\right)S\left(a,q,\frac{\varphi}{2}\right) - C\left(a,q,\frac{\varphi}{2}\right)\dot{S}\left(a,q,\frac{\varphi}{2}\right) = \quad (5)$$

$$\dot{C}(a,q,0)S(a,q,0) - C(a,q,0)\dot{S}(a,q,0) =$$

$$-C(a,q,0)\dot{S}(a,q,0) = P(a,q)$$

As was demonstrated in [5], the $P(a,q)$ function is useful for mapping of the stability boundaries where it is equal to zero. The value of $P(a,q)$ is a real number only for a stable trajectory. The contour plot of the $P(a,q)$ function values for the first stability region was depicted using x and y directions in [5]. Figure 1 represents the same for the second stability region. The amplitude $|P(a,q)^{-1}|$ also reflects the trajectory size and approaches infinity on the stability boundary ($P(a,q) = 0$, dashed lines). The boundaries computed using the equivalence of the Mathieu characteristic exponent to 0 and 1 coincide with $P(a,q) = 0$ boundaries.

An equivalent, but in some cases preferable, presentation of the solution of the Mathieu differential equation can be obtained as follows:

$$x(t) = K_1 S\left(a,q,\frac{\omega t}{2}+\frac{\varphi}{2}\right) + K_2 C\left(a,q,\frac{\omega t}{2}+\frac{\varphi}{2}\right) \quad (6)$$

$$\dot{x}(t) = \frac{\omega}{2}\left(K_1\dot{S}\left(a, q, \frac{\omega t}{2} + \frac{\varphi}{2}\right) + K_2\dot{C}\left(a, q, \frac{\omega t}{2} + \frac{\varphi}{2}\right)\right)$$

where $K_{1,2}$ are

$$\begin{cases} K_1 = \dfrac{1}{P(a, q)}\left(-2\dfrac{\dot{x}_i}{\omega}C\left(a, q, \dfrac{\varphi}{2}\right) + x_i\dot{C}\left(a, q, \dfrac{\varphi}{2}\right)\right) \\ K_2 = \dfrac{1}{P(a, q)}\left(2\dfrac{\dot{x}_i}{\omega}S\left(a, q, \dfrac{\varphi}{2}\right) - x_i\dot{S}\left(a, q, \dfrac{\varphi}{2}\right)\right) \end{cases} \text{ or}$$

$$\begin{cases} K_1 = \dfrac{2\dfrac{\dot{x}_i}{\omega}}{\dot{S}(a, q, 0)} \text{ for } \varphi = 0. \\ K_2 = \dfrac{x_i}{C(a, q, 0)} \end{cases} \quad (7)$$

The $\varphi = 0$ case is considered in this work to compare the derived ion energy with other results [4, 6]. In this instance for ions injected on the quadrupole axis ($x_i = 0$, $K_2 = 0$ or parallel to it ($\dot{x}_i = 0$, $K_1 = 0$), a trajectory is accepted provided the following conditions are met:

$$\frac{x(t)}{r_0} = \frac{2\dot{x}_i}{\omega r_0}\frac{S\left(a, q, \frac{\omega t}{2}\right)}{\dot{S}(a, q, 0)} < 1 \text{ or}$$

$$\frac{x(t)}{r_0} = \frac{x_i}{r_0}\frac{C\left(a, q, \frac{\omega t}{2}\right)}{C(a, q, 0)} < 1,$$

respectively.

Quadrupole Trap

For the quadrupole ion trap [7, 8] we have:

$$\Phi = \frac{(x^2 + y^2 - 2z^2)}{2r_0^2}(U - V\cos(\omega t + \varphi)). \quad (8)$$

The system of equations of ion motion with initial conditions $\{x_i, y_i, z_i\}$ and $\{\dot{x}_i, \dot{y}_i, \dot{z}_i\}$ in Cartesian system of coordinates is given as:

$$\begin{cases} m\ddot{x}(t) = -e\dfrac{x(t)}{r_0^2}(U - V\cos(\omega t + \varphi)) \\ m\ddot{y}(t) = -e\dfrac{y(t)}{r_0^2}(U - V\cos(\omega t + \varphi)), \\ m\ddot{z}(t) = e\dfrac{2z(t)}{r_0^2}(U - V\cos(\omega t + \varphi)) \end{cases}$$

$$\begin{cases} x(0) = x_i; \dot{x}(0) = \dot{x}_i \\ y(0) = y_i; \dot{y}(0) = \dot{y}_i \\ z(0) = z_i; \dot{z}(0) = \dot{z}_i, \end{cases} \quad (9)$$
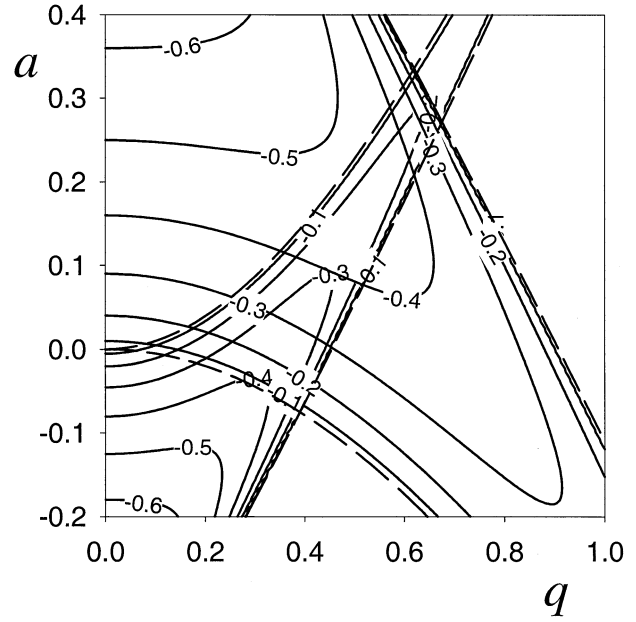

Figure 2. Diagram of stability of ion trajectories in the quadrupole trap for the first region calculated employing $P(a, q)$ function (see eq 5). Dashed lines represent $P(a, q) = 0$, which also coincide with boundaries calculated with help of the Mathieu characteristic exponent.

where r_0 is the ring electrode radius. We consider the case where $z_0 = \dfrac{r_0}{\sqrt{2}}$ is the half spacing between the end caps.

Although the ion trap as well as $\{x_i, y_i, z_i\}$ have cylindrical symmetry (x and y coordinates are degenerate), the $\{\dot{x}_i, \dot{y}_i, \dot{z}_i\}$ initial conditions do not possess the same symmetry and for $\dot{x}_i$ and $\dot{y}_i$ coordinates the degeneracy is not present (the quadrupole trap $\dot{x}(t)$, $\dot{y}(t)$ and $\dot{z}(t)$ are different). The corresponding formal solution of equation of motion for the x and y directions are given by eq 3, and for the z direction we have:

$$z(t) = \frac{1}{P(-2a, -2q)}$$

$$\times\left[2\frac{\dot{z}_i}{\omega}Q\left(-2a, -2q, \frac{\omega t}{2}, \frac{\varphi}{2}\right) + z_i L\left(-2a, -2q, \frac{\omega t}{2}, \frac{\varphi}{2}\right)\right],$$

$$\dot{z}(t) = \frac{1}{P(-2a, 2q)} \quad (10)$$

$$\times\left[\dot{z}_i QP\left(-2a, -2q, \frac{\omega t}{2}, \frac{\varphi}{2}\right) + z_i\frac{\omega}{2}LP\left(-2a, -2q, \frac{\omega t}{2}, \frac{\varphi}{2}\right)\right].$$

The first region of stability is represented in Figure 2, where the x and z directions were employed to map the stability boundaries.

Investigation of Ion Energy in the Presence of the RF-Field

In the absence of collisions, ion energy variations occur as a result of interaction with the RF quadrupole field. The ion trajectory eqs 3 and 10 are used in this investigation. It is evident from the systems of differential eqs 2 and 9 that there is no energy exchange between the velocity components and they should be considered independently. They are also homologous and the investigation of one component is applicable to all. Coupling of energy between different degrees of freedom could be activated by collisions or by the presence of multipole components in the quadrupole field; this will also be examined separately in a following publication.

First, let us consider the approximate solution similar to Gerlich [6] for the ion potential energy $\varepsilon_x(t)$. To estimate the energy of an ion $E_x(t)$ in the quadrupole field, we assume that $\varphi = 0$, $a = 0$, q is small, and initial speed $\dot{x}_i$ is small enough to prevent $x(t)$ reaching r_0. Therefore, for the ion energy we have:

$$
\frac{2E_x(t)}{m} = \dot{x}(t)^2 = \frac{\omega^2 x_i^2}{4}\left(\frac{\dot{C}\left(0, q, \frac{\omega t}{2}\right)}{C(0, q, 0)}\right)^2
$$

$$
+ x_i\dot{x}_i\omega\frac{\dot{C}\left(0, q, \frac{\omega t}{2}\right)\dot{S}\left(0, q, \frac{\omega t}{2}\right)}{C(0, q, 0)\dot{S}(0, q, 0)}
$$

$$
+ \dot{x}_i^2\left(\frac{\dot{S}\left(0, q, \frac{\omega t}{2}\right)}{\dot{S}(0, q, 0)}\right)^2 \tag{11}
$$

The time-averaged values of the included functions for small values of the q parameter are:

$$
\left\langle\left(\frac{\dot{C}\left(0, q, \frac{\omega t}{2}\right)}{C(0, q, 0)}\right)^2\right\rangle_{\omega t} = 0,
$$

$$
\left\langle\frac{\dot{C}\left(0, q, \frac{\omega t}{2}\right)\dot{S}\left(0, q, \frac{\omega t}{2}\right)}{C(0, q, 0)\dot{S}(0, q, 0)}\right\rangle_{\omega t} = 0, \tag{12}
$$

$$
\left\langle\left(\frac{\dot{S}\left(0, q, \frac{\omega t}{2}\right)}{\dot{S}(0, q, 0)}\right)^2\right\rangle_{\omega t} = 1
$$

and $\frac{2}{m}E_x = \frac{2}{m}\langle E_x(t)\rangle_{\omega t} = \langle\dot{x}(t)^2\rangle_{\omega t} = \dot{x}_i^2$, which demonstrates conservation of the ion energy on average for the assumed restrictions on a, q, $\dot{x}_i$, and φ. The contribution of the quadrupole field into the potential energy can be estimated from the expansion series:

$$
\frac{\omega^2 x_i^2}{4}\left(\frac{\dot{C}\left(0, q\to 0, \frac{\omega t}{2}\right)}{C(0, q\to 0, 0)}\right)^2
$$

$$
= \frac{\omega^2 x_i^2}{4}\left(\dot{C}^{(0,1,0)}\left(0, q\to 0, \frac{\omega t}{2}\right)\right)^2 q^2 + O(q^3). \tag{13}
$$

Note, that the first term in the expansion is equal to zero. The time-averaged value for the second term is:

$$
\left\langle\left(\dot{C}^{(0,1,0)}\left(0, q\to 0, \frac{\omega t}{2}\right)\right)^2\right\rangle_{\omega t} = \frac{1}{2}
$$

and

$$
\varepsilon_x = \langle\varepsilon_x(t)\rangle_{\omega t} = \frac{1}{16} m\omega^2 x_i^2 q^2 = \frac{e^2 V^2}{4m\omega^2 r_0^2}\left(\frac{x_i}{r_0}\right)^2, \tag{14}
$$

per degree of freedom, which is equal to the results obtained by Gerlich [6] for the quadrupole field [assuming the definition (eq 1) of the RF amplitude]. For the linear quadrupole and quadrupole ion trap, the potential ion energy are given by:

$$
\varepsilon_r = \langle\varepsilon_x(t)\rangle_{\omega t} + \langle\varepsilon_y(t)\rangle_{\omega t} = \frac{e^2 V^2}{4m\omega^2 r_0^2}\left(\frac{r_i}{r_0}\right)^2 \text{ and}
$$

$$
\varepsilon = \langle\varepsilon_x(t)\rangle_{\omega t} + \langle\varepsilon_y(t)\rangle_{\omega t} + \langle\varepsilon_z(t)\rangle_{\omega t}
$$

$$
= \frac{e^2 V^2}{4m\omega^2 r_0^2}\left(\left(\frac{r_i}{r_0}\right)^2 + \left(\frac{z_i}{z_0}\right)^2\right), \tag{15}
$$

respectively. Here $r_i^2 = x_i^2 + y_i^2$.

A comprehensive analysis requires more information about the initial ion velocity distribution function. The Maxwell-Boltzmann (MB) distribution function is adopted here. This distribution function is elliptically symmetric around the stream (macroscopic) velocity and the most probable values of the thermal (microscopic) velocity components are zero. It is reasonable to expect that the initial radial ion stream velocity is negligible (the ion beam is coaxial with the linear quadrupole field or macroscopically motionless in the ion trap).

Assuming that $\dot{x}_i$ is distributed according to the MB distribution:

$$
f(\dot{x}_i) = \frac{\gamma_\perp}{\sqrt{\pi}}\exp(-\gamma_\perp^2\dot{x}_i^2), \tag{16}
$$

the most probable ion thermal speed $\frac{1}{\gamma_\perp}$ in the RF affected direction is related to the initial radial translational kinetic temperature $T_\perp$ in the same direction as follows:

$$\frac{\gamma_\perp}{\sqrt{\pi}} \int_{-\infty}^{\infty} \dot{x}_i^2 \exp(-\gamma_\perp^2 \dot{x}_i^2) d\dot{x}_i = \frac{1}{2\gamma_\perp^2} = RT_\perp;$$

$$\gamma_\perp = \frac{1}{\sqrt{2RT_\perp}}; \quad R = k_B/m, \tag{17}$$

where k_B is the Boltzmann's constant.

Under the RF-field, $\dot{x}_i$ is transformed into $\dot{x}$. Some helpful integrals and functions of a, q, ωt, and φ can be introduced:

$$v_{21}^2(a, q, \omega t, \varphi) = \frac{1}{P(a, q)^2} LP\left(a, q, \frac{\omega t}{2}, \frac{\varphi}{2}\right)^2;$$

$$v_{21}^2(a, q, \omega t) = \langle v_{21}^2(a, q, \omega t, \varphi)\rangle_\varphi,$$

$$v_{21}^2(a, q, \varphi) = \langle v_{21}^2(a, q, \omega t, \varphi)\rangle_{\omega t},$$

$$v_{21}^2(a, q) = \langle\langle v_{21}^2(a, q, \omega t, \varphi)\rangle_\varphi\rangle_{\omega t} \tag{18}$$

$$v_{22}^2(a, q, \omega t, \varphi) = \frac{1}{P(a, q)^2} QP\left(a, q, \frac{\omega t}{2}, \frac{\varphi}{2}\right)^2;$$

$$v_{22}^2(a, q, \omega t) = \langle v_{22}^2(a, q, \omega t, \varphi)\rangle_\varphi,$$

$$v_{22}^2(a, q, \varphi) = \langle v_{22}^2(a, q, \omega t, \varphi)\rangle_{\omega t},$$

$$v_{22}^2(a, q) = \langle\langle v_{22}^2(a, q, \omega t, \varphi)\rangle_\varphi\rangle_{\omega t}. \tag{19}$$

The functions (eqs 18 and 19) are averaged (integrated and normalized) over φ, ωt or both.

The fraction of the RF-driven ions having radial velocity $\dot{x}$ which were originated within a velocity space element $d\dot{x}_i$ at $\dot{x}_i$ that have their energy within an energy element dE at E and can be presented as:

$$\frac{2dE}{m} = \frac{\gamma_\perp}{\sqrt{\pi}} \left(\frac{1}{P(a, q)}\left[\dot{x}_i QP\left(a, q, \frac{\omega t}{2}, \frac{\varphi}{2}\right)\right.\right.$$

$$\left.\left. + x_i \frac{\omega}{2} LP\left(a, q, \frac{\omega t}{2}, \frac{\varphi}{2}\right)\right]\right)^2 \exp(-\gamma_\perp^2 \dot{x}_i^2) d\dot{x}_i. \tag{20}$$

Therefore, for the affected component of the ion energy in the presence of the RF field we obtain the following equation:

$$\frac{2E_x(t)}{m} = \frac{\gamma_\perp}{\sqrt{\pi}} \int_{-\infty}^{\infty} \left(\frac{1}{P(a, q)}\left[\dot{x}_i QP\left(a, q, \frac{\omega t}{2}, \frac{\varphi}{2}\right)\right.\right.$$

$$\left.\left. + x_i \frac{\omega}{2} LP\left(a, q, \frac{\omega t}{2}, \frac{\varphi}{2}\right)\right]\right)^2 \exp(-\gamma_\perp^2 \dot{x}_i^2) d\dot{x}_i$$
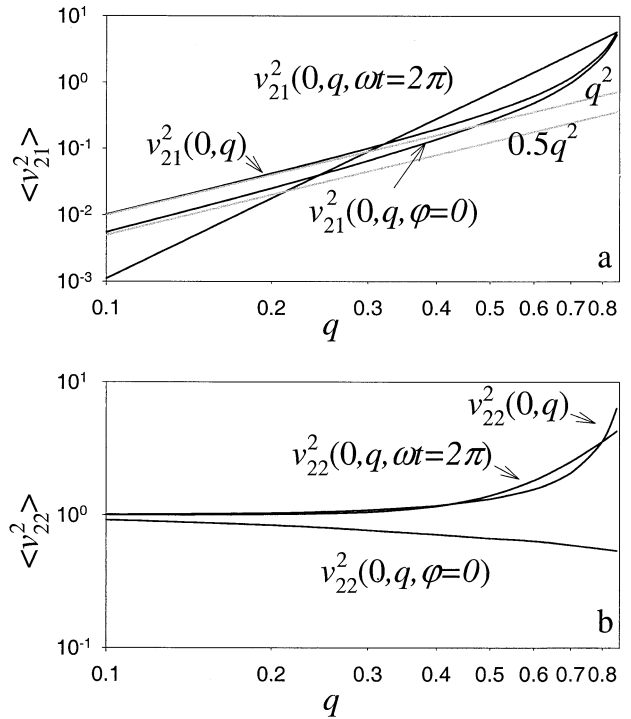

Figure 3. (**a**) Comparison of approximate solution $\frac{1}{2}q^2$ and q^2 with integrals $v_{21}^2(0, q)$, $v_{21}^2(0, q, \varphi = 0)$, and $v_{21}^2(0, q, \omega t = 2\pi)$ as a function of the q parameter. (**b**) $v_{22}^2(0, q)$, $v_{22}^2(0, q, \varphi = 0)$, and $v_{22}^2(0, q, \omega t = 2\pi)$ as functions of the q parameter.

$$= \frac{\omega^2 x_i^2}{4} v_{21}^2(a, q, \omega t, \varphi) + \frac{1}{2\gamma_\perp^2} v_{22}^2(a, q, \omega t, \varphi) \tag{21}$$

and for time and phase averaged energy:

$$E_x = \frac{m\omega^2}{8} x_i^2 v_{21}^2(a, q) + \frac{m}{4\gamma_\perp^2} v_{22}^2(a, q). \tag{22}$$

In the particular case of the RF only ion guide ($a = 0$) the radial ion energy can be introduced similar to eq 15:

$$E_r = \frac{m\omega_2}{8} r_i^2 v_{21}^2(0, q) + \frac{m}{2\gamma_\perp^2} v_{22}^2(0, q). \tag{23}$$

Here both components of the ion energy are presented: Potential (proportional to x_i^2, which is quite similar to eq 14 and Gerlich [6]) and kinetic (proportional to $\frac{1}{\gamma_\perp^2}$). Direct comparison with eq 23 reveals that $v_{21}^2(0, q, \varphi = 0) \approx \frac{1}{2}q^2$ (here $v_{21}^2(0, q, \omega t, \varphi)$ is averaged over time for $\varphi = 0$). In Figure 3a different levels of $v_{21}^2(0, q, \omega t, \varphi)$ averaging and approximate solutions are plotted together making clear the limits of the approximation (eq 14).

Eq 14 for the potential ion energy was developed

Table 1. Values of special and averaged solutions of integrals (18) and (19) for selected a and q parameters

a	q	$v_{21}^2(a, q, \omega t)$ $\omega t=2\pi$	$v_{22}^2(a, q, \omega t)$ $\omega t=2\pi$	$v_{21}^2(a, q)$	$v_{21}^2(a, q, \varphi)$ $\varphi=0$	$v_{22}^2(a, q, \varphi)$ $\varphi=0$	$v_{22}^2(a, q)$
0	0.1	1.11033−3	1.0007	0.0101	5.5114e−3	0.9179	1.0085
0	0.2	0.0178	1.0104	0.0419	0.0250	0.8384	1.0370
0	0.3	0.0899	1.0523	0.1009	0.0655	0.7685	1.0912
0	0.4	0.2842	1.1648	0.1981	0.1383	0.7128	1.1800
0	0.5	0.6937	1.4010	0.3570	0.2660	0.6674	1.3243
0	0.6	1.4383	1.8281	0.6277	0.4948	0.6362	1.5666
0	0.7	2.6643	2.5262	1.1900	0.9966	0.5937	2.0864
0	0.8	4.5444	3.5893	2.8348	2.5086	0.5547	3.6084
0	0.85	5.7910	4.2896	5.7998	5.2644	0.5377	6.3499
0.236994	0.708996	6.4771	2.8671				
−0.236994	0.705996	1.0943	4.4051				
0.0295495	5.5472754	64832	2376.7				
−0.0295495	7.5472754	66990	2464.8				
3.164296	3.234075	96.3728	6.5189				
2.5209999	2.8153045	85.152	6.2444				

assuming the time average values for $\varphi = 0$ only, which is not quite satisfactory. This is also evident in the $v_{22}^2(0, q, \varphi = 0)$ dependence (the ion kinetic energy) on the q parameter. Low RF field influence is expected then $\langle v_{21}^2 \rangle \to 0$ and $\langle v_{22}^2 \rangle \to 1$, which is consistent with the conservation of the ion kinetic energy. However, the resultant $v_{22}^2(0, q, \varphi = 0)$ values are less than unity corresponding to an artificial (unrealistic) cooling of the ions. Nevertheless, having been derived from similar assumptions, the potential ion energy $\frac{\omega^2 x_i^2}{4} v_{21}^2(0, q, \varphi = 0)$ and eq 14 are in agreement.

A detailed picture of the ion energy can be obtained from the analysis of integrals (18,19), which represent dimensionless multipliers for evaluation of the ion potential and kinetic energy. At the present moment, the time-averaged values of the integrals cannot be reliably calculated close to a stability boundary due to an essential singularity ($|P(a, q)^{-1}|$ rapidly approaches 0^{-1}). However, the special solutions collected in Table 1 are sufficiently representative of the contribution of the RF field to the ion energy at the stability boundaries. It is also important to remember that this analysis is limited to a single RF affected translational degree of freedom of the ion motion according to eq 22. The total effect should be calculated as a superposition of independent contributions similar to eq 15 and can be presented as eq 23 only for the RF ion guide. It is also interesting to note that $v_{21}^2(a, q, \omega t = 2\pi)$ over the wide range of q values corresponding to the normal operation range of the RF only ion guide.

In Figure 4 black contour lines represent $v_{21}^2(a, q, \omega t = 2\pi)$ and gray lines represent $v_{22}^2(a, q, \omega t = 2\pi)$. "Low q and $a = 0$ " conditions annul the first integral and the second is very close to unity. Starting from $q > 0.5$ both integrals have similar values between 1 and 10. With injection of ions close to the quadrupole axis, first term diminishes. At the tip of the stability diagram ($a = 0.236994$, $q = 0.705996$) the first integral is equal to 2.8671 and the second is equal to 3.4771. Contributions

in other regions of stability are presented in Table 1, which demonstrates together with Figure 3b that averaging over the phase φ is required.

Therefore, in order to acquire the potential ion energy one has to know the dimensionless parameter (integral) $v_{21}^2(a, q)$, which depends only on the RF field properties. For the ion kinetic energy, value of the $v_{22}^2(a, q)$ parameter is required. Table 2 presents calculated ion energy components compared to the approximate solution. For example, for an ion with mass $m = 250$ Da and with radial temperature $T_\perp = 10^3$K (0.043 eV, for a single degree of freedom), which starts with position r_i in the quadrupole field ($a = 0$, $q = 0.4$, $\omega =$
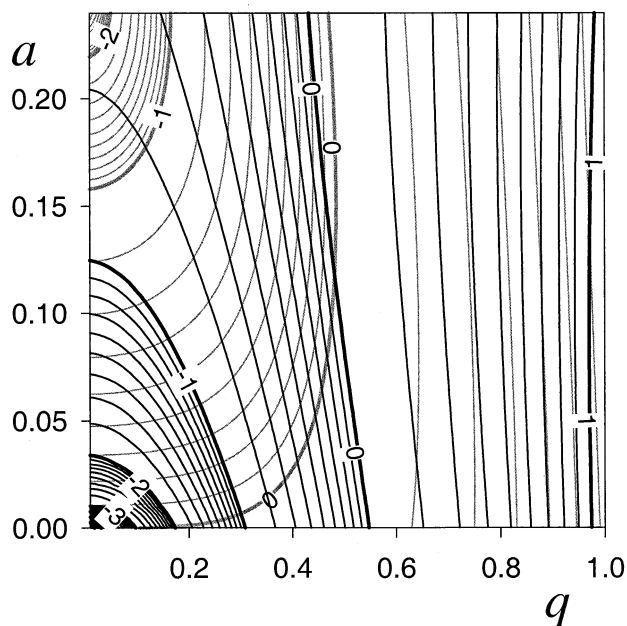

Figure 4. Contour plot of some integrals (eqs 18 and 19) on the a vs. q space. Only exponents are used as marks (0 corresponds to the integral value 1). Black contour lines represent integral $v_{21}^2(a, q, \omega t = 2\pi)$ and gray lines–$v_{22}^2(a, q, \omega t = 2\pi)$.

Table 2. Examples of contribution of the potential and kinetic components into the ion energy. In all cases the a parameter is equal to 0, radial translational temperature $T_\perp = 10^3 K$, initial position $r_i = 0.25 r_0$ in the quadrupole field with $\omega = 2\pi$MHz, $r_0 = 4.1$ mm

m, Da	q	$\dfrac{e^2 V^2}{4m\omega^2 r_0^2}\left(\dfrac{r_i}{r_0}\right)^2$, eV	$\dfrac{m\omega^2}{8} r_i^2 v_{21}^2(0, q)$, eV	$\dfrac{m}{2\gamma_\perp^2} v_{22}^2(0, q)$, eV	E_r, eV
40	0.2	0.04	0.09	0.09	0.18
40	0.4	0.17	0.43	0.1	0.53
40	0.85	0.78	12.47	0.55	13.01
250	0.2	0.27	0.56	0.09	0.65
250	0.4	1.07	2.66	0.1	2.76
250	0.85	4.85	77.92	0.55	78.47
1000	0.2	1.07	2.25	0.09	2.34
1000	0.4	4.3	10.65	0.1	10.75
1000	0.85	19.41	311.69	0.55	312.23

2π MHz, $r_0 = 4.1$ mm), the E_r energy (according to eq 23) is equal to 2.76 eV. More examples for different ions under similar conditions are presented in Table 2.

It is expected that an increase in the contribution of the RF-field to the ion energy should lead to a decrease in transmission/acceptance. It should also result in an increase in the centre-of-mass energy of ion–neutral collisions. For example, as can be seen from Table 1, special care should be given to matching the emittance of an ion source and acceptance of a quadrupole in the alternative stability regions (II and III), where a better vacuum is also required. As a remedy, one can try focusing ions just on the quadrupole axis (even if they diverge later on), which should reduce the RF contribution to the ion energy.

Conclusions

The contribution of the RF field to the ion energy depends on the a and q parameters and this dependence is considered in detail. In order to evaluate the average ion energy in the quadrupole RF field, one has to calculate the dimensionless parameters $v_{21}^2(a, q)$ and $v_{22}^2(a, q)$, which depend only on the field properties. It has been shown that the analytical solution of the Mathieu equation in conjunction with the algebraic presentation of Mathieu functions yields reliable method for these calculations that agree with approximate solution for the ion potential energy. The ion energy is considered for different stability regions. The $v_{21}^2(a, q)$ and $v_{22}^2(a, q)$ parameters are tabulated partially

in this work along with simple formulae for their calculation for any a and q parameters.

References

1. Frenkel, D.; Portugal, R. Algebraic Methods to Compute Mathieu Functions. *J. Phys. A Math. Gen.* **2001,** *34,* 3541–3551.
2. Kokkorakis, G. C.; Roumeliotis, J. A. Power Series Expansions for Mathieu Functions with Small Arguments. *Math. Comput.* **2001,** *70,* 1221–1235.
3. O'Dell, D. H. J. Dynamical Diffraction in Sinusoidal Potentials: Uniform Approximations for Mathieu Functions. *J. Phys. A Math. Gen.* **2001,** *34,* 3897–3925.
4. Ioanoviciu, D. Ion Trajectories in Quadrupole Mass Filters for a and q Parameters Near the Stability Region Tip. *Rapid Commun. Mass Spectrom.* **1997,** *11,* 1383–1386.
5. Baranov, V. I. Analytical Approach for Description of an Ion Motion in Quadrupole Mass Spectrometry. *J. Am. Soc. Mass Spectrom.* **2003,** *14,* 818–824.
6. Gerlich, D. Inhomogeneous RF Fields: A Versatile Tool for the Study of Processes with Slow Ions. In *State-Selected and State-to-State Ion-Molecule Reaction Dynamics, Part I. Experiment*, Adv. Chem. Physics Series, Vol LXXXII; Ng, C.-Y.; Baer, M., Eds.; LXXXII ed.; Wiley and Sons: Hoboken, NJ; 1992; pp 1–176.
7. March, R. E.; Hughes, R. J. Quadrupole Storage Mass Spectrometry; John Wiley and Sons: New York, 1989.
8. March, R. E. An Introduction to Quadrupole Ion Trap Mass Spectrometry. *J. Am. Soc. Mass Spectrom.* **1997,** *32,* 351–369.